

Electronic Supplementary Information for

Modulating extraction and retention of fluorinated β -diketonate metal complexes in perfluorocarbons through the use of non-fluorinated neutral ligands

Tyler L. King[‡], Orhi Esarte Palomero[‡], Dawson A. Grimes[‡], Sean T. Goralski[‡], Richard A. Jones[‡], Emily L. Que^{*‡}

[‡] The University of Texas at Austin, Department of Chemistry, 1 University Station A5300, Austin, Texas, 78712, United States

Table of Contents	Page(s)
Experimental procedures	S2-5
Table S1. Experimental parameters for CW X-band EPR spectra	S6
Table S2. EasySpin simulation parameters for Cu(L) ₂ and derivatives	S6
Table S3. Structural parameters of Zn(L) ₂ (H ₂ O) ₂ , Zn(acac) ₂ (H ₂ O) ₂ , and Zn(hfa) ₂ (H ₂ O) ₂	S7
Table S4. Magnetic parameters of Cu(L) ₂ , Cu(L) ₂ (Py) ₂ , and Cu(L) ₂ TMEDA in PFCE	S7
Figure S1. Job's continuous variance plots for Mn ²⁺ , Fe ³⁺ , Co ²⁺ , Ni ²⁺ , Cu ²⁺ , Zn ²⁺ , Ga ³⁺ , In ³⁺ , and Pb ²⁺	S8
Figure S2. Job's continuous variance plots for Sc ³⁺ , Y ³⁺ , La ³⁺ , Nd ³⁺ , Eu ³⁺ , Gd ³⁺ , Lu ³⁺ , Th ⁴⁺ , and UO ₂ ²⁺	S9
Figure S3. Absorbance spectrum of Ni(L) ₂ in PFCE	S10
Figure S4. Crystal structure of Zn(L) ₂ (H ₂ O) ₂	S10
Figure S5. Crystalline packing of Zn(L) ₂ (H ₂ O) ₂	S11
Figure S6. Crystal structure of Mn(L) ₂ (H ₂ O) ₂	S11
Figure S7. Crystalline packing of Mn(L) ₂ (H ₂ O) ₂	S12
Figure S8. CW X-band EPR of Cu(L) ₂ in PFCE at 115 K	S12
Figure S9. Neutral nitrogen donor ligands examined as synergistic extractants	S13
Figure S10. Absorbance spectrum of Ni(L) ₂ in PFCE with varying amounts of pyridine added	S14
Figure S11. Absorbance spectrum of Ni(L) ₂ in PFCE with varying amounts of tetramethylethylenediamine (TMEDA) added	S14
Figure S12. CW X-band EPR of Cu(L) ₂ , Cu(L) ₂ (Py) ₂ , and Cu(L) ₂ TMEDA in PFCE	S15
Figure S13. ¹⁹ F NMR of LH , Eu(L) ₃ , Eu(L) ₃ + Py, and Eu(L) ₃ + TMEDA	S16
References	S17

Experimental

All chemicals used were obtained from commercial sources and used without further purification. Perfluoro-15-crown-5 ether (PFCE) was obtained from Exflour Research Corp. (Round Rock, Texas). **LH** was obtained from SynQuest Laboratories (Alachua, Florida). Metal salts used for aqueous phase preparation for all extractions are listed below. ^{19}F NMR spectroscopic measurements of metal-doped PFCE were taken with a coaxial insert filled with D_2O for locking purposes using an Agilent MR 400 NMR spectrometer at 376 MHz and room temperature. Inductively coupled plasma optical emission spectrometry (ICP-OES) was performed on a Varian 710 Series ICP-OES in the EWRE lab in the Department of Civil, Architectural and Environmental Engineering at the University of Texas at Austin. UV-Vis absorbance spectra were taken using a Agilent Cary 60 UV-Vis spectrophotometer.

Metal Ion	Metal Salt Used	Supplier
Li^+	LiCl	Fisher Scientific
Na^+	NaCl	Fisher Scientific
K^+	KCl	Fisher Scientific
Rb^+	RbCl	Fisher Scientific
Cs^+	CsCl	Fisher Scientific
Mg^{2+}	MgCl_2	Fisher Scientific
Ca^{2+}	CaCl_2	Fisher Scientific
Sr^{2+}	$\text{SrCl}_2 \cdot 6\text{H}_2\text{O}$	Alfa Aesar
Ba^{2+}	$\text{BaCl}_2 \cdot 2\text{H}_2\text{O}$	Fisher Scientific
Mn^{2+}	$\text{MnCl}_2 \cdot 4\text{H}_2\text{O}$	Strem
Fe^{3+}	$\text{FeCl}_3 \cdot 6\text{H}_2\text{O}$	Mallinckrodt
Co^{2+}	$\text{CoCl}_2 \cdot 6\text{H}_2\text{O}$	Acros
Ni^{2+}	$\text{NiCl}_2 \cdot 6\text{H}_2\text{O}$	Acros
Cu^{2+}	$\text{CuCl}_2 \cdot 2\text{H}_2\text{O}$	Acros
Zn^{2+}	$\text{Zn(OAc)}_2 \cdot 2\text{H}_2\text{O}$	Fisher Scientific
Zr^{4+}	$\text{ZrOCl}_2 \cdot 8\text{H}_2\text{O}$	Aldrich
Ru^{3+}	$\text{RuCl}_3 \cdot \text{XH}_2\text{O}$	Sigma Aldrich
Rh^{3+}	$\text{RhCl}_3 \cdot 3\text{H}_2\text{O}$	Pressure Chem
Pd^{2+}	$\text{Pd}(\text{NO}_3)_2$	Aldrich
Ag^+	AgNO_3	Sigma Aldrich
Cd^{2+}	CdCl_2	Sigma Aldrich
Ir^{3+}	$\text{IrCl}_3 \cdot 3\text{H}_2\text{O}$	Sigma Aldrich
Pt^{2+}	K_2PtCl_4	Sigma Aldrich
Ga^{3+}	$\text{Ga}(\text{NO}_3)_3$	Alfa Aesar
In^{3+}	InCl_3	Strem
Pb^{2+}	$\text{Pb}(\text{NO}_3)_2$	Mallinckrodt
Sc^{3+}	$\text{Sc}(\text{OTf})_3$	Alfa Aesar
Y^{3+}	$\text{Y}(\text{NO}_3)_3$	Lindsay Chemical Company
La^{3+}	$\text{La}(\text{OTf})_3$	Sigma Aldrich
Nd^{3+}	$\text{Nd}(\text{OTf})_3$	Sigma Aldrich
Eu^{3+}	$\text{Eu}(\text{OTf})_3$	Sigma Aldrich
Gd^{3+}	$\text{Gd}(\text{OTf})_3$	Sigma Aldrich
Tb^{3+}	$\text{Tb}(\text{OTf})_3$	Sigma Aldrich
Dy^{3+}	$\text{Dy}(\text{OTf})_3$	Sigma Aldrich
Yb^{3+}	$\text{Yb}(\text{OTf})_3$	Sigma Aldrich
Lu^{3+}	$\text{Lu}(\text{OTf})_3$	Sigma Aldrich
Th^{4+}	$\text{Th}(\text{NO}_3)_4$	Strem
UO_2^{2+}	$\text{UO}_2(\text{OAc})_2 \cdot 2\text{H}_2\text{O}$	JT Baker

Extraction of metal ions into the fluorous phase

For monovalent metal ions, a solution of **LH** in PFCE (400 μ L, 10 mM) was added to an aqueous solution of the metal salt (400 μ L, 10 mM, 100 mM MES pH 6) in a 1.5 mL Eppendorf tube. The biphasic mixture was mixed for 30 minutes using a Labquake Shaker Rotisserie. The biphasic mixture was then centrifuged (3,000 rcf, 3 min) to separate the aqueous and fluorous phases. The aqueous phase was diluted with 2% HNO_3 and the metal content was determined via ICP-OES. For M^{n+} ions the concentration of **LH** in PFCE was increased to $n*10$ mM. Due to precipitation of metal salts of Fe^{3+} , Ga^{3+} , and Ru^{3+} during aqueous phase preparation with pH 6 MES buffer, the following buffers were used for aqueous phase preparation of these ions: Fe^{3+} - 100 mM acetate buffer pH 5; Ga^{3+} 100 mM HEPES buffer pH 8; Ru^{3+} 100 mM acetate buffer pH 4.

Leaching of metal ions from fluorous phase with HNO_3

The fluorous phase from each forward extraction (125 μ L) was added to 1M HNO_3 (2.5 mL) and mixed with a Benchmark Scientific H2024 incubator shaker at 40°C using the mix setting for 24 hrs. The biphasic mixture was then centrifuged (3,000 rcf, 3 min) to separate the aqueous and fluorous phases. The aqueous phase was diluted with 2% HNO_3 and the metal content was determined via ICP-OES. The same protocol was used for leaching of metal ions synergistically extracted with nitrogen donors.

Leaching of metal ions from fluorous phase with HEPES Buffer

A solution of $M^{n+}(L)_n$ in PFCE was synthesized using the same extraction procedure and standardized to 5 mM metal ion concentration in the fluorous phase. Metal-doped PFCE (500 μ L) was added to 100 mM HEPES buffer (500 μ L, pH 7.4, 100 mM NaCl) in a 1.5 mL Eppendorf tube. The biphasic mixture was mixed with a Benchmark Scientific H2024 incubator shaker at 37°C using the mix setting for 24 hrs. The biphasic mixture was then centrifuged (3,000 rcf, 3 min) to separate the aqueous and fluorous phases. The aqueous phase was diluted 100x with 2% HNO_3 and the metal content was determined via ICP-OES. The same protocol was used for leaching of metal ions synergistically extracted with nitrogen donors.

Leaching of metal ions from fluorous phase with EDTA

A solution of $M^{n+}(L)_n$ in PFCE was synthesized using the same extraction procedure and standardized to 5 mM metal ion concentration in the fluorous phase. Metal-doped PFCE (500 μ L) was added to 100 mM HEPES buffer (500 μ L, pH 7.4, 100 mM NaCl, 50 mM EDTA) in a 1.5 mL Eppendorf tube. The biphasic mixture was mixed with a Benchmark Scientific H2024 incubator shaker at 37°C using the mix setting for 24 hrs. The biphasic mixture was then centrifuged (3,000 rcf, 3 min) to separate the aqueous and fluorous phases. The aqueous phase was diluted with 2% HNO_3 and the metal content was determined via ICP-OES. The same protocol was used for leaching of metal ions synergistically extracted with nitrogen donors.

Synergistic extraction of metal ions with nitrogen donors

Extractions were carried out as described above with the addition of nitrogen donor ligands. The amount of nitrogen donor added to the extraction mixture was based on the number of expected open coordination sites of the metal ion and the denticity of the nitrogen donor. E.g., 1.5 equivalents of pyridine were added for each expected open coordination site, so 3 equivalents pyridine relative to Ni^{2+} . For bi- and tri-dentate nitrogen donors 1.5 equivalents was added relative to M^{n+} .

X-ray crystallography

X-ray diffraction experiments were performed in the University of Texas at Austin X-Ray Diffraction Laboratory. Single crystals were selected using a microscope, coated in Paratone oil and mounted on nylon loops.

Crystallographic data was acquired in an Agilent Supernova diffractometer equipped with an AtlasS2 CCD using collimating mirror monochromators with μ -focus $\text{CuK}\alpha$ radiation ($\lambda = 1.5418 \text{ \AA}$) or $\text{MoK}\alpha$ ($\lambda = 0.71073 \text{ \AA}$) radiation at 100 K, provided by an Oxford 700 series Cryostream device. Data was reduced and absorption corrected with the aid of the Agilent Technologies CrysAlysPro V 1.171.37.31 software.

Structures were solved using Olex2¹, by SHELXS² or SHELXT³ and refined with full-matrix least-squares calculations on $F2$ by using SHELXL.⁴ Non-hydrogen atoms were refined anisotropically and hydrogen atoms were included in the refinement using a riding model. ORTEP diagrams were created using Olex2.

Specific details regarding the refinement of each structure can be found in the corresponding .cif files. These files were deposited in the Cambridge Crystallographic Data Centre (deposition number 2091566 and 2091567). These files can be obtained free of charge via www.ccdc.cam.ac.uk/data_request/cif, or by emailing data_request@ccdc.cam.ac.uk, or by contacting The Cambridge Crystallographic Data Centre, 12 Union Road, Cambridge CB2 1EZ, UK; fax: +44 1223 336033.

Luminescence lifetime measurements

Luminescence lifetimes of Eu^{3+} -doped PFCE solutions were obtained on a QuantaMaster 4 photon technology international (PTI) instrument. Luminescent decays of the 615 nm emission of Eu^{3+} was measured after excitation of the sample at 320 nm. Each decay was fitted as a single exponential decay with a χ^2 between 0.9 and 1.1.

Acquisition and Simulation of CW X-band EPR Spectra

Solutions of $\text{Cu}(\text{L})_2$, $\text{Cu}(\text{L})_2(\text{Py})_2$, and $\text{Cu}(\text{L})_2\text{TMEDA}$ in PFCE were prepared using extraction procedures described above, loaded into 4 mm quartz EPR tubes, and then flash-frozen in liquid nitrogen. All spectra were obtained on a Bruker EMX EPR spectrometer equipped with an EMX

high-sensitivity probehead. All spectra were acquired using the parameters listed in Table S1. Spectra were simulated using the EasySpin software.⁵ The specific parameters input for each simulation are given in Table S2.

Equations for extraction equilibria and distribution ratio calculations

The equilibrium for the extraction of neutral metal complexes with variable nuclearity assuming only anionic **L** ligands is given by Equation S1.



$$K_{ex} = [M_a L_{a+n}]_{fl} / [M^{n+}]^a [L^-]^{a+n}$$

S1

The distribution ratio, *D*, of the metal ion between the fluorous and aqueous phases is therefore given by Equation S2.

$$D = \frac{[M^{n+}]_{fl, total}}{[M^{n+}]_{aq, total}} = \frac{\sum_a a [M_a L_{a+n}]_{fl}}{\sum_b [ML_b^{a-b}]_{aq}} = \frac{\sum_a a K_{ex} [M^{n+}]^{a-1} [L^-]^{a+n}}{\sum_b \beta_b [L^-]^b}$$

S2

Where β_b is the stability constant given by Equation S3.

$$\beta_b = [ML_b^{n-b}]_{aq} / [M^{n+}] [L^-]^b$$

S3

Table S1. Experimental parameters for CW X-band EPR spectra.

Receiver Gain	2.00E+03
Phase	0 deg
Harmonic	1
Modulation Frequency	100.000 kHz
Modulation Amplitude	4.000 G
Conversion Time	9.000 ms
Time Constant	5.120 ms
Sweep Time	45.000 s
Microwave Frequency	9.40 GHz
Microwave Power	0.1262 mW
Resolution in x	5000
Center Field	3200.000 G
Sweep Width	2000.000 G
Temperature	115.0 K

Table S2. EasySpin parameters for simulated EPR spectra.

	CuL₂	CuL₂+py	CuL₂+TMEDA
S	1/2	1/2	1/2
g_x	2.055	2.113	2.092
g_y	2.055	2.113	2.092
g_z	2.293	2.273	2.278
Nucleus	Cu	Cu	Cu
A_x, MHz	55	12	37
A_y, MHz	55	12	37
A_z, MHz	498	564	525
g-strain_x	0.01	0.07	0.06
g-strain_y	0.01	0.07	0.06
g-strain_z	0.02	0.12	0.10
Microwave Frequency, GHz	9.42427	9.42427	9.42427
Temperature, K	115	115	115

Table S3. Structural parameters for $\text{Zn}(\text{L})_2(\text{H}_2\text{O})_2$, $\text{Zn}(\text{hfac})_2(\text{H}_2\text{O})_2$ ⁶ and $\text{Zn}(\text{acac})_2(\text{H}_2\text{O})_2$ ⁷. The structural parameters of $[\text{Zn}^{2+}(\text{L})_2(\text{H}_2\text{O})_2]$ resemble those of the known $[\text{Zn}(\text{acac})_2(\text{H}_2\text{O})_2]$ and $[\text{Zn}(\text{hfac})_2(\text{H}_2\text{O})_2]$.

Compound	$[\text{Zn}(\text{L})_2(\text{H}_2\text{O})_2]$	$\text{Zn}(\text{hfac})_2(\text{H}_2\text{O})_2$ ⁶	$\text{Zn}(\text{acac})_2(\text{H}_2\text{O})_2$ ⁷
Bond Lengths (Å)			
Zn-O1	2.034(2)	2.052	2.0319(8)
Zn-O2	2.070(2)	2.061	2.0492(8)
Zn-OH ₂	2.145(2)	2.099	2.1849(8)
Angles (°)			
$\angle \text{O1-Zn-O2}$	88.58(9)	88.991	90.53(3)

Table S4. Magnetic parameters of $\text{Cu}(\text{L})_2$, $\text{Cu}(\text{L})_2(\text{Py})_2$, $\text{Cu}(\text{L})_2\text{TMEDA}$, and previously reported $\text{Cu}(\text{acac})_2$ complexes determined by CW X-band EPR and simulations. Ligand abbreviations: acac = acetylacetone, hfacac = hexafluoroacetylacetone, bpy = 2,2'-bipyridine, en = ethylenediamine.

Compound	\mathbf{g}_{\parallel}	\mathbf{g}_{\perp}	\mathbf{A}_{\parallel} , MHz	\mathbf{A}_{\perp} , MHz
$\text{Cu}(\text{acac})_2^1$	2.285	2.060	520	35
$\text{Cu}(\text{hfacac})_2(\text{bpy})^1$	2.299	2.056	486	77
$\text{Cu}(\text{acac})(\text{en})^1$	2.184	2.033	621	77
$\text{Cu}(\text{L})_2$	2.293	2.055	498	55
$\text{Cu}(\text{L})_2(\text{Py})_2$	2.273	2.113	546	12
$\text{Cu}(\text{L})_2\text{TMEDA}$	2.278	2.092	525	37

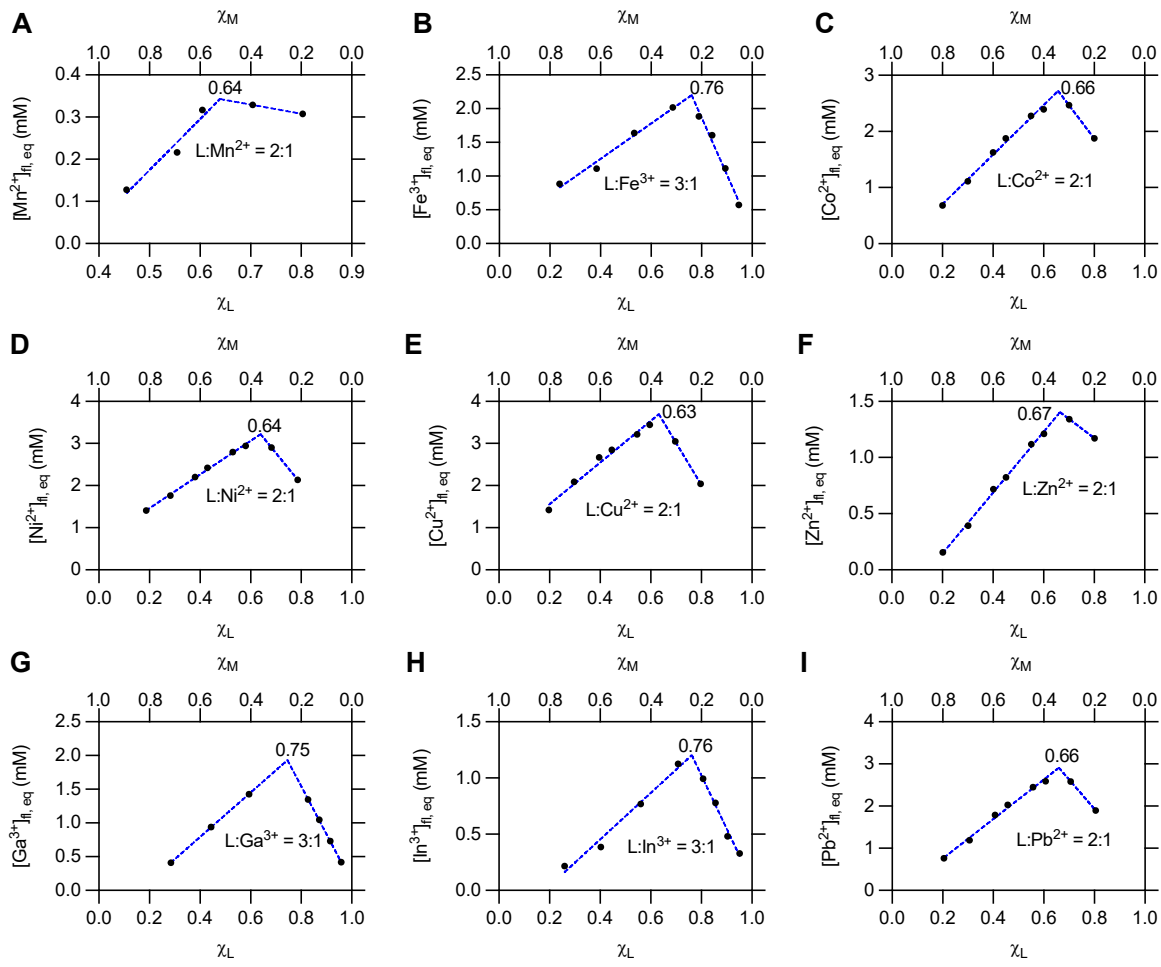


Figure S1. Job's continuous variance plots of for Mn^{2+} (A), Fe^{3+} (B), Co^{2+} (C), Ni^{2+} (D), Cu^{2+} (E), Zn^{2+} (F), Ga^{3+} (G), In^{3+} (H), and Pb^{2+} (I) with LH . $[LH]_{fl, ini} + [M^{n+}]_{aq, ini} = 10$ mM (100 mM MES buffer pH 6 for all metal ions except Fe^{3+} (100 mM acetate buffer pH 5) and Ga^{3+} (100 mM HEPES buffer pH 8)). Extraction time = 30 mins. Mole fractions of LH and M^{n+} indicated as χ_L and χ_M respectively.

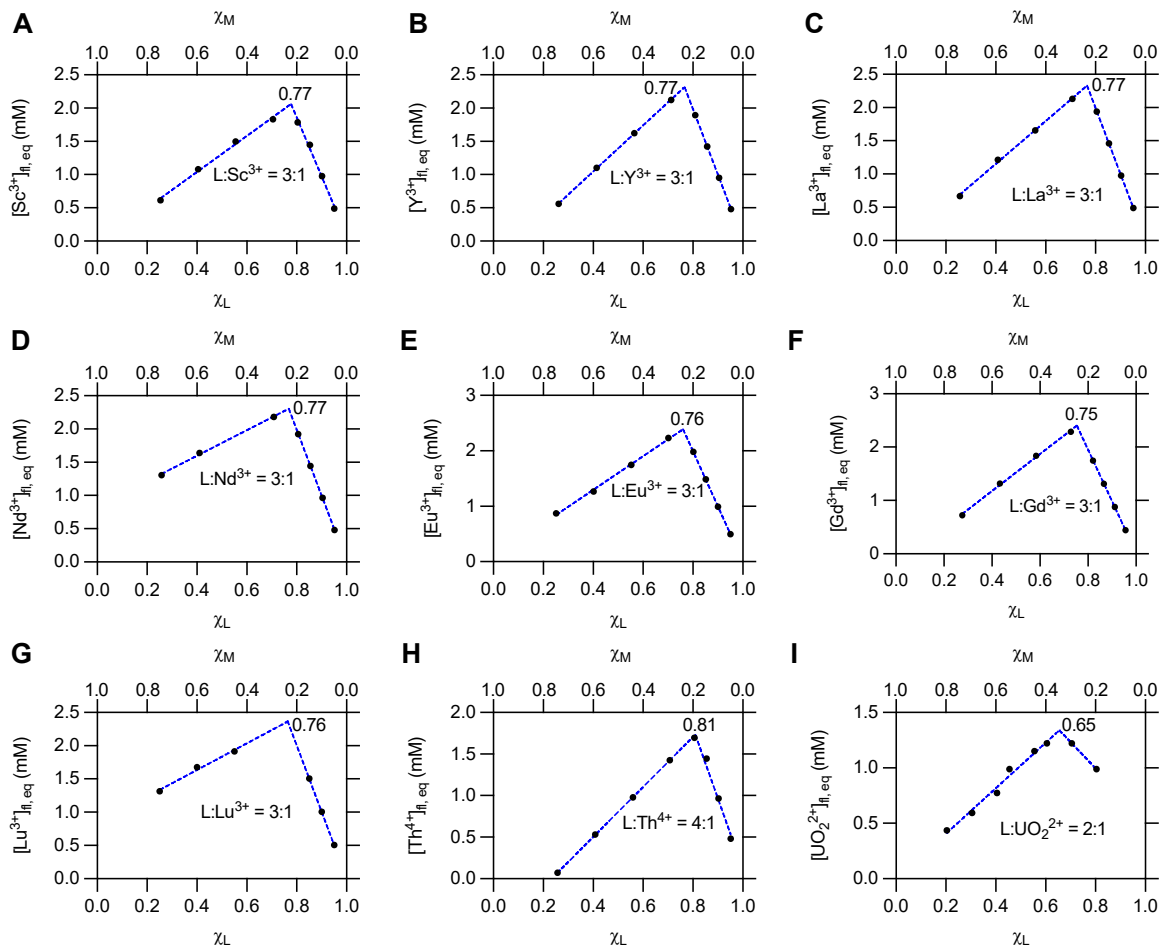


Figure S2. Job's continuous variance plots of for Sc³⁺ (A), Y³⁺ (B), La³⁺ (C), Nd³⁺ (D), Eu³⁺ (E), Gd³⁺ (F), Lu³⁺ (G), Th⁴⁺ (H), and UO₂²⁺ (I) with LH. $[\text{LH}]_{\text{fl, ini}} + [\text{M}^{n+}]_{\text{aq, ini}} = 10 \text{ mM}$ (100 mM MES buffer pH 6 for all metal ions). Extraction Time = 30 mins. Mole fractions of LH and Mⁿ⁺ indicated as χ_L and χ_M respectively.

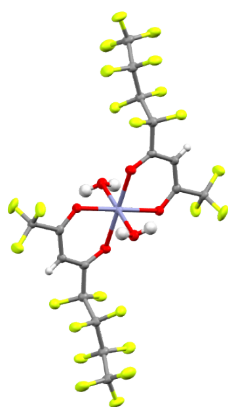


Figure S3. Crystal structure of $\text{Zn}(\text{L})_2(\text{H}_2\text{O})_2$. Thermal ellipsoid plots at 50 % probability are shown. Metal complex $[\text{Zn}^{2+}(\text{L})_2(\text{H}_2\text{O})_2]$ is octahedral and crystallizes as colorless crystalline planks in the P-1 space group. In the solid-state the aquo ligand are trans to each other while the two L^- ligands occupy the equatorial plane.

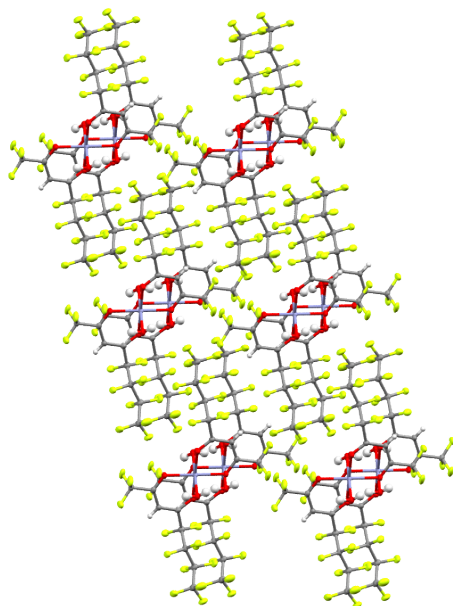


Figure S4. Packing of $\text{Zn}(\text{L})_2(\text{H}_2\text{O})_2$ showing segregation of perfluorinated C_4F_9 chains and ZnO_6 units. The packing of the $\text{Zn}(\text{L})_2(\text{H}_2\text{O})_2$ structure is characterized by assembly of the perfluorinated C_4F_9 chains while the Zn acac core forms a linear hydrogen bonded network enabled by the acac oxygens and the water ligands. Thermal ellipsoid plots at 50 % probability are shown.

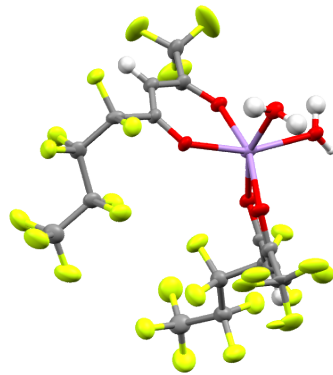


Figure S5. Crystal structure of $\text{Mn}(\text{L})_2(\text{H}_2\text{O})_2$. Thermal ellipsoid plots at 50 % probability are shown. Compound $[\text{Mn}^{2+}(\text{L})_2(\text{H}_2\text{O})_2]$ forms yellow needles in the P-1 space group. In this case, the aquo ligands are *cis* in the six-coordinate metal complex.

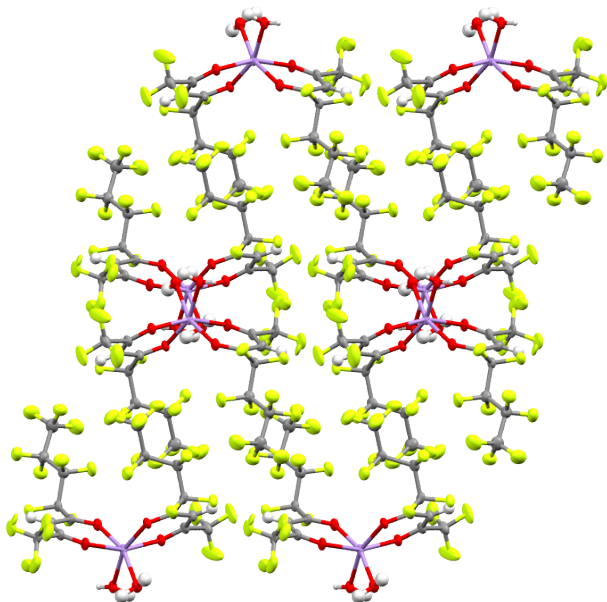


Figure S6. Packing of $\text{Mn}(\text{L})_2(\text{H}_2\text{O})_2$ showing segregation of perfluorinated C_4F_9 chains and MnO_6 units. The C_4F_9 substituents assemble together while the Mn acac coordination sphere is held in place by hydrogen bonding interactions with between alternating Mn acac units. Thermal ellipsoid plots at 50 % probability are shown.

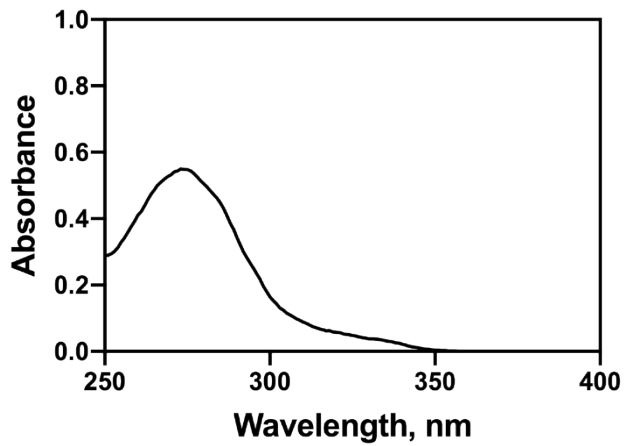


Figure S7. UV-vis absorbance spectrum of $\text{Ni}(\text{L})_2$ in PFCE, $[\text{Ni}^{2+}] = 10 \mu\text{M}$.

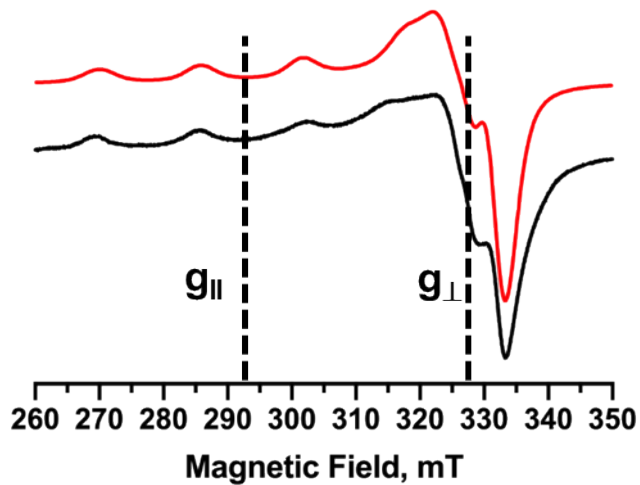


Figure S8. CW X-band EPR spectrum (black) of $\text{Cu}(\text{L})_2$ acquired in frozen solution of PFCE (20 mM) at 115 K along with the simulated spectrum (red).

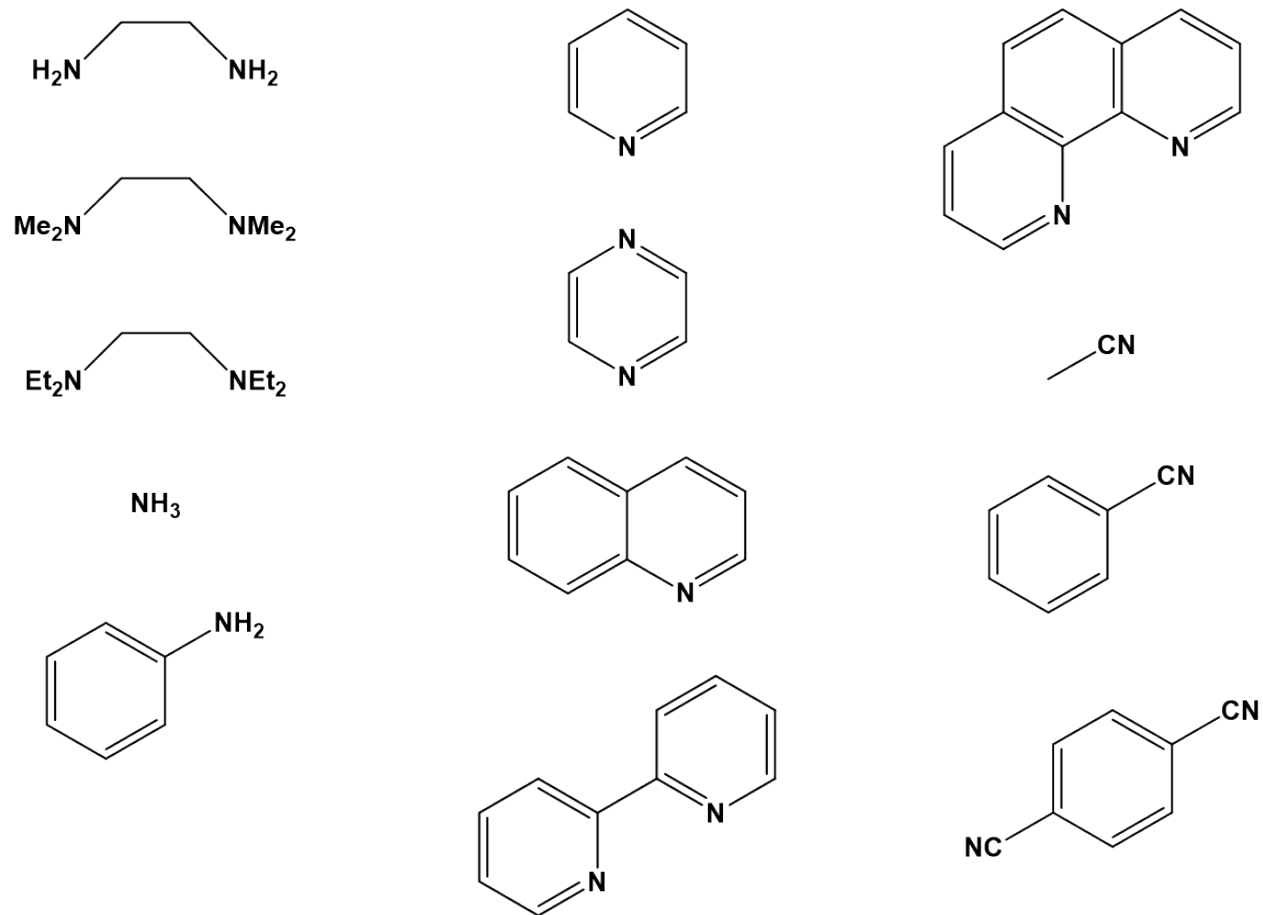


Figure S9. Nitrogen donor ligands (**A**) examined as synergistic extractants for Ni^{2+} .

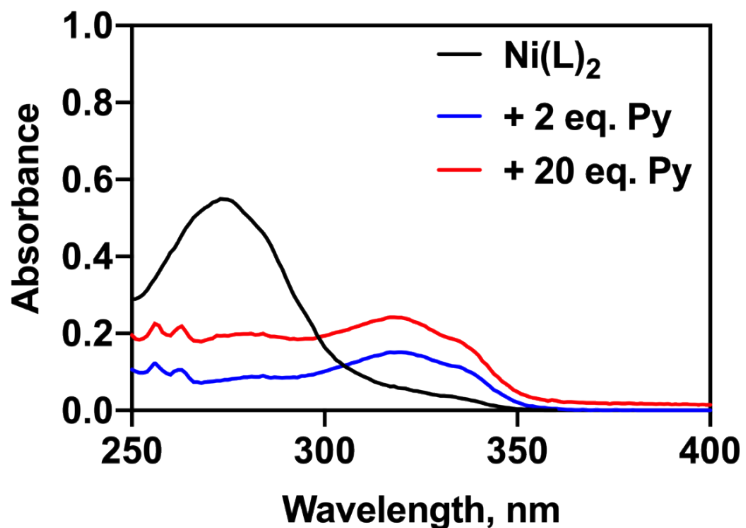


Figure S10. Absorbance spectra of $\text{Ni}(\text{L})_2$ in PFCE with increasing amounts of pyridine (Py) added during extraction, $[\text{Ni}^{2+}] = 10 \mu\text{M}$.

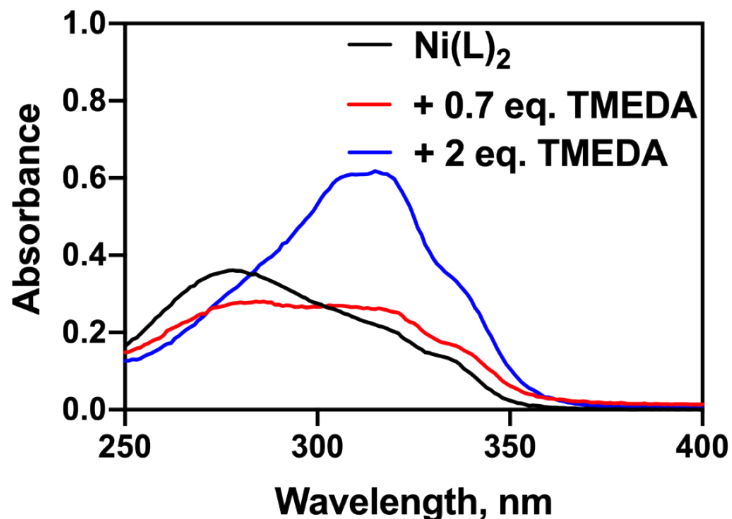


Figure S11. UV-vis absorbance spectra of $\text{Ni}(\text{L})_2$ in PFCE with increasing amounts of tetramethylethylenediamine (TMEDA) added during extraction, $[\text{Ni}^{2+}] = 10 \mu\text{M}$.

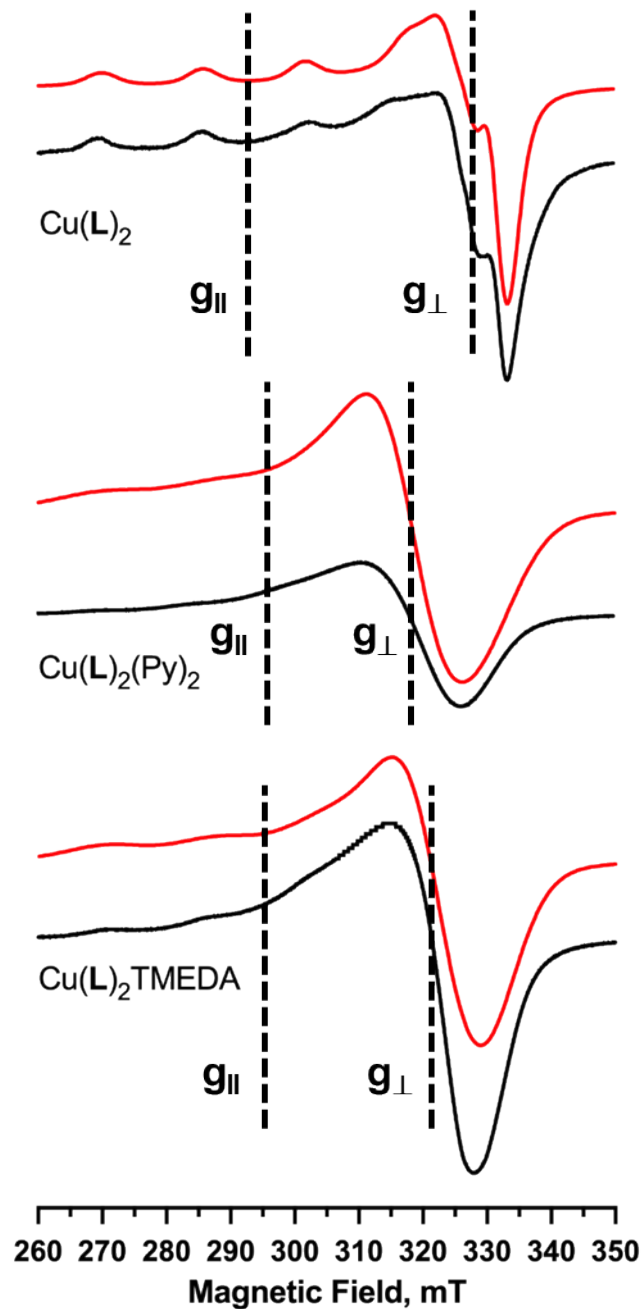


Figure S12. CW X-band EPR spectra (black) of $\text{Cu}(\text{L})_2$, $\text{Cu}(\text{L})_2(\text{Py})_2$, and $\text{Cu}(\text{L})_2\text{TMEDA}$ acquired in frozen solution of PFCE (20 mM) at 115 K along with their respective simulated spectra (red).

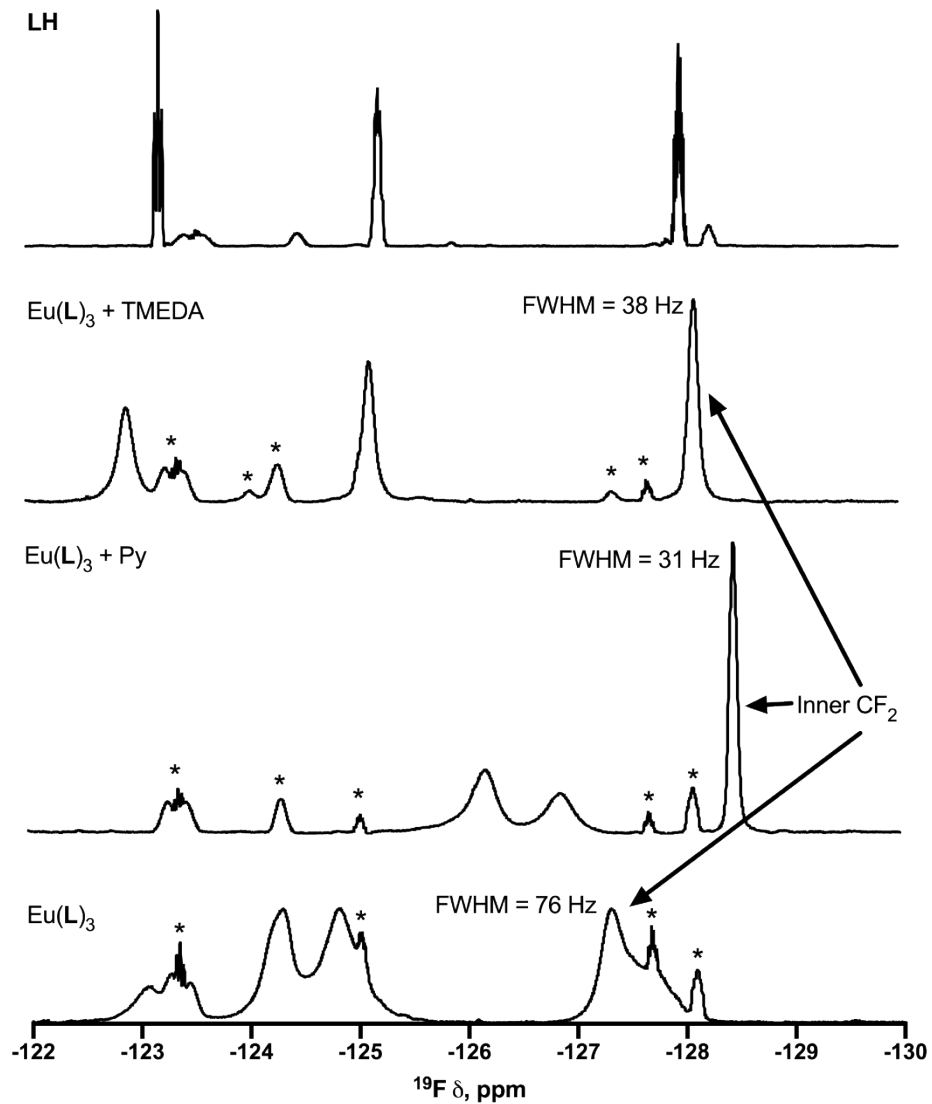


Figure S13. ^{19}F NMR spectrum (376 MHz, neat, 25°C) of **LH** in PFCE (10 mM) and the $\text{Eu}(\text{L})_3$ species extracted with only **LH**, **LH** + 60 mM pyridine, and **LH** + 20 mM TMEDA. $[\text{Eu}^{3+}]_{\text{f}} = 10 \text{ mM}$. Py = pyridine. TMEDA = tetramethylethylenediamine. Note, a coaxial insert filled with D_2O was used for solvent locking.

References

- 1 O. V. Dolomanov, L. J. Bourhis, R. J. Gildea, J. A. K. Howard and H. Puschmann, OLEX2: A complete structure solution, refinement and analysis program, *J. Appl. Crystallogr.*, 2009, **42**, 339–341.
- 2 G. M. Sheldrick, A short history of SHELX, *Acta Crystallogr. Sect. A Found. Crystallogr.*, 2008, **64**, 112–122.
- 3 G. M. Sheldrick, SHELXT - Integrated space-group and crystal-structure determination, *Acta Crystallogr. Sect. A Found. Crystallogr.*, 2015, **71**, 3–8.
- 4 G. M. Sheldrick, Crystal structure refinement with SHELXL, *Acta Crystallogr. Sect. C Struct. Chem.*, 2015, **71**, 3–8.
- 5 S. Stoll and A. Schweiger, EasySpin, a comprehensive software package for spectral simulation and analysis in EPR, *J. Magn. Reson.*, 2006, **178**, 42–55.
- 6 P. Harbach, H. W. Lerner and M. Bolte, Diaquadiacetylacetatozinc(II), *Acta Crystallogr. Sect. E Struct. Reports Online*, 2003, **59**, 724–725.
- 7 R. P. Adams, H. C. Allen, R. Urszula and D. J. Hodgson, The EPR Spectrum of Mn(II) Doped into cis-Diaquobis(1,1,1,5,5,5-hexafluoroacetylacetato)zinc(II) and trans-Diaquobis(1,1,1,5,5,5-hexafluoroacetylacetato)zinc(II) and the Crystal Structure of the Host Crystals, *Inorganica Chim. Acta Chem.*, 1986, **119**, 67–74.